ACKNOWLEDGMENTS

The research leading to these results received funding from the European Union Seventh Framework Programme (FP7/2007-2013) under grant agreement no. 298935 to Y.H. and has been supported by the U.S. National Science Foundation (NSF) Long-Term Ecological Research (LTER) Program at Cedar Creek (DEB-8811884, DEB-9411972, DEB-0080382, DEB-0620652, and DEB-1234162), Biocomplexity Coupled Biogeochemical Cycles (DEB-0322057), Long-Term Research in Environmental Biology (DEB-0716587, DEB-1242531), and Ecosystem Sciences (NSF DEB-1120064) Programs, as well as the U.S. Department of Energy (DOE) Program for Ecosystem Research (DE-FG02-96ER62291) and the U.S. DOE National Institute for Climatic Change Research (DE-FC02-06ER64158). We thank T. Mielke, D. Bahauddin, K. Worm, S. Barrott, E. Lind, and many summer interns for their assistance with this research. We also thank R. S. L. Veiga, W. S. Harpole, T. Züst, and M. Tanadini for suggestions that improved the manuscript. For detailed methods and original data, see www.cedarcreek.umn.edu/research/data. See table S1 for links to data for each experiment and supplementary materials for guidance on data access. The authors declare no conflict of interests. Author contributions: Y.H. and D.T. developed and framed the research question; D.T., F.I., E.W.S., E.T.B., and P.B.R. designed research; D.T., E.W.S., E.T.B., and P.B.R. performed research; Y.H. and F.I. analyzed data; and Y.H. wrote the paper with inputs from all coauthors.

SUPPLEMENTARY MATERIALS

www.sciencemag.org/content/348/6232/336/suppl/DC1
Materials and Methods
Figs. S1 and S2
Tables S1 to S4
References (*32*–*39*)

5 November 2014; accepted 23 February 2015
10.1126/science.aaa1788

STEM CELLS

Asymmetric apportioning of aged mitochondria between daughter cells is required for stemness

Pekka Katajisto,[1,2,3,4]*† Julia Döhla,[4] Christine L. Chaffer,[1] Nalle Pentinmikko,[4] Nemanja Marjanovic,[1,2] Sharif Iqbal,[4] Roberto Zoncu,[1,2,3] Walter Chen,[1,2,3] Robert A. Weinberg,[1,2] David M. Sabatini[1,2,3,5,6]*

By dividing asymmetrically, stem cells can generate two daughter cells with distinct fates. However, evidence is limited in mammalian systems for the selective apportioning of subcellular contents between daughters. We followed the fates of old and young organelles during the division of human mammary stemlike cells and found that such cells apportion aged mitochondria asymmetrically between daughter cells. Daughter cells that received fewer old mitochondria maintained stem cell traits. Inhibition of mitochondrial fission disrupted both the age-dependent subcellular localization and segregation of mitochondria and caused loss of stem cell properties in the progeny cells. Hence, mechanisms exist for mammalian stemlike cells to asymmetrically sort aged and young mitochondria, and these are important for maintaining stemness properties.

Stem cells can divide asymmetrically to generate a new stem cell and a progenitor cell that gives rise to the differentiated cells of a tissue. During organismal aging, it is likely that stem cells sustain cumulative damage, which may lead to stem cell exhaustion and eventually compromise tissue function (*1*). To slow the accumulation of such damage, stem cells might segregate damaged subcellular components away from the daughter cell destined to become a new stem cell. Although nonmammalian organisms can apportion certain non-nuclear cellular compartments (*2*–*4*) and oxidatively damaged proteins (*5*, *6*) asymmetrically during cell division, it is unclear whether mammalian stem cells can do so as well (*6*–*9*).

We used stemlike cells (SLCs) recently identified in cultures of immortalized human mammary epithelial cells (*10*) to investigate whether mammalian stem cells can differentially apportion aged, potentially damaged, subcellular components, such as organelles between daughter cells. These SLCs express genes associated with stemness, form mammospheres, and, after transformation, can initiate tumors in vivo (*10*, *11*). Moreover, because of their round morphology, the SLCs can be distinguished by visual inspection from the flat, tightly adherent, nonstemlike mammary epithelial cells with which they coexist in monolayer cultures (Fig. 1B).

To monitor the fate of aged subcellular components, we expressed photoactivatable green fluorescent protein (paGFP) (*12*) in lysosomes, mitochondria, the Golgi apparatus, ribosomes, and chromatin by fusing the fluorescent protein to the appropriate targeting signals or proteins (table S1). paGFP fluoresces only after exposure to a pulse of ultraviolet (UV) light (*12*), allowing us to label each component in a temporally controlled manner (Fig. 1A). Because synthesis of paGFP continues after the light pulse, cells subsequently accumulate unlabeled "young" components in addition to the labeled "old" components; these can be either segregated in distinct subcellular compartments or commingled within individual cells.

We followed the behavior of labeled components in single round SLCs or flat epithelial cells and focused on cell divisions that occurred 10 to 20 hours after paGFP photoactivation (Fig. 1B). The epithelial cells symmetrically apportioned all cellular components analyzed (Fig. 1B). In contrast, the round SLCs apportioned ~5.6 times as much ($P < 0.001$, t test) of ≥10-hour-old mitochondrial outer membrane protein 25 (paGFP-Omp25) to one daughter cell as to the other (Fig. 1B). Similarly, labeled markers for all other organelles examined were apportioned symmetrically. We designated the daughter cell that inherited more aged Omp25 from the mother cell as Progeny1 (P1) and the other as Progeny2 (P2).

To determine whether the same cells that asymmetrically apportion the mitochondrial membrane protein also allocate other membrane compartments asymmetrically, we labeled SLCs with the lipophilic dye PKH26 before photoactivation of paGFP-Omp25. PKH26 initially labels the plasma membrane and is gradually endocytosed to form distinct cytoplasmic puncta, and it is relatively symmetrically apportioned during division of hematopoietic cells (*13*). SLCs apportioned old mitochondria asymmetrically, but the same cells apportioned PKH26 symmetrically (Fig. 1C and movie S1). In contrast, the epithelial cells apportioned both paGFP-Omp25 and PKH26 symmetrically (Fig. 1C and movie S2), similarly to mouse embryonic fibroblasts (not shown).

To verify that SLCs indeed apportion mitochondria according to the age of the organelle, we analyzed the apportioning of paGFP-Omp25 in cell divisions that occurred at random times after the initial photoactivation. We assumed that the age of Omp25 molecules reflected the age of the mitochondria with which they were associated. Cells that divided 0 to 10 hours after photoactivation showed symmetric apportioning of paGFP-Omp25 (Fig. 1D). However, cells that divided more than 10 hours after photoactivation, and thus carried fluorescent marks only on organelles that were at least 10 hours old, apportioned their labeled mitochondria asymmetrically (Fig. 1D).

To follow the apportioning of two different age classes of mitochondria, we tagged mitochondria with mitochondrial proteins fused to a Snap-tag (*14*). Snap-tag is a derivatized DNA repair enzyme, O^6-alkylguanine-DNA alkyltransferase, which can covalently link various fluorophores to the tagged fusion protein in live cells. We used two Snap-tag substrates with two different fluorophores (red

[1]Whitehead Institute for Biomedical Research, Boston, MA 02142, USA. [2]Department of Biology, Massachusetts Institute of Technology (MIT), Cambridge, MA 02139, USA. [3]Howard Hughes Medical Institute, MIT, Cambridge, MA 02139, USA. [4]Institute of Biotechnology, University of Helsinki, P.O. Box 00014, Helsinki, Finland. [5]Broad Institute, Cambridge, MA 02142, USA. [6]The David H. Koch Institute for Integrative Cancer Research at MIT, Cambridge, MA 02139, USA.
*Corresponding author. E-mail: pekka.katajisto@helsinki.fi (P.K.); sabatini@wi.mit.edu (D.M.S.) †Present address: Institute of Biotechnology, University of Helsinki, P.O. Box 00014, Helsinki, Finland.

and green) sequentially to separately label young and old organelles (Fig. 2A). Snap-tags are rendered inactive by the labeling reaction; this ensures that the two colors will mark chronologically distinct populations and, in contrast to previously used strategies (*15*), allows precise timing of labeling. Moreover, Snap-tags allow uniform labeling throughout the entire cell and the simultaneous labeling of multiple cells and avoid the risk of phototoxic artifacts associated with paGFP (*16*).

We analyzed divisions of SLCs expressing Snap-Omp25 and carrying red and green fluorophores on what we refer to as old and young mitochondria, labeled 48 to 58 and 0 to 10 hours before division, respectively (Fig. 2B and movie S3). After cell division, the old label from the mother cell was divided more asymmetrically between daughter cells than the young label (old: P1 89% versus P2 11% of the mother cell intensity, $P = 0.004$; young: 67% versus 33%, $P = 0.04$, $n = 5$) (Fig. 2, B and C, and fig. S1). This age-specific apportioning reduced the relative portion of old mitochondria in P2 to about one-fifth of those in the mother cell and one-sixth of those in the P1 daughter (fig. S2A). However, cells that inherited fewer old mitochondria contained similar total amounts of mitochondria (fig. S3), suggesting that unlabeled new mitochondria generated after the "young labeling" were differentially distributed to balance the overall mitochondrial quantity between the two daughters. We also targeted the mitochondrial inner membrane (see fig. S4 for mitochondrial constructs used) by expressing COX8A-Snap in SLCs. This inner membrane protein showed asymmetric distribution comparable to that of Omp25 (Fig. 2C), increasing our confidence that the age-selective segregation of Omp25 represented that of whole mitochondria.

Our analyses of asymmetric cell divisions indicated that the majority of mitochondria in the stemlike mother cells contained both old and young labels, whereas some mitochondria carried only young or old label (Fig. 2B). Most mitochondria carrying exclusively young label apportioned to the P2 daughter cells, whereas mitochondria containing a mix of the two labels segregated to P1 cells (Fig. 2B). Moreover, the small quantity of old label received by P2 did not colocalize with young label (Fig. 2B and fig. S2B). These findings indicate that even before cell division, the stemlike mother cell keeps new mitochondria apart from old ones and passes these younger mitochondria preferentially to the P2 daughter.

To study such segregation in greater detail, we analyzed SLCs immediately after labeling of the young mitochondria but before division (fig. S5 and Fig. 2D). Old mitochondria tended to localize perinuclearly and in some cells formed puncta containing exclusively old label (figs. S5 and S6), whereas the young label distributed throughout the mitochondrial network more evenly. To address whether such localization differences could contribute to the demonstrated age-specific apportioning, we imaged old and young mitochondria with live microscopy within the 10-hour window we used for analyses of asymmetric division (Fig. 2E). Young (green) label gradually became more perinuclear as it became older, but at 10 hours after labeling, which was the maximum time point used for the quantitation of asymmetry in cell division, there was still a significant difference in the localization of the two labels (Fig. 2E). The perinuclear localization of old label did not occur in a fibroblast cell line without stemlike properties (fig. S6), and it did not result from old label entering and marking other subcellular components, such as lysosomes, due to mitochondrial turnover (fig. S7). However, within the interconnected mitochondrial network, we identified specific domains that were enriched for old label (Fig. 2D). These data support the notion that mother SLCs localize new and old mitochondria to specific cytoplasmic regions, ostensibly to facilitate the exclusion of old mitochondria from future P2 daughter cells.

The asymmetric apportioning and localization of mitochondria in the daughter cells suggested that daughter cells resulting from a division of a SLC might represent the founders of two lineages, one stemlike and the other more likely to differentiate. We used flow cytometry to analyze the age-selective apportioning of mitochondria in cell populations that had been synchronized to divide in concert (fig. S8 and Fig. 3A). Some divided cells received significantly fewer old mitochondria than did others, whereas the young mitochondria were more uniformly distributed. Upon fluorescence-activated cell sorting (FACS) and replating of daughter cell populations, the Pop1 cells, which received more old mitochondria, were morphologically flatter and more adherent than the Pop2 cells (Fig. 3A). Three days after cell sorting, the Pop1 cells formed clusters with a monolayer appearance, whereas the Pop2 cells regenerated both round and flat cells similar to the original parental population. However, both populations had similar rates of proliferation (fig. S9). Thus, Pop2 cells, which received fewer older mitochondria, appeared to represent the SLCs that could subsequently undergo asymmetric divisions.

We used the ability to form mammospheres in three-dimensional (3D) culture as an in vitro assay of mammary epithelial cell stemness (*17*).

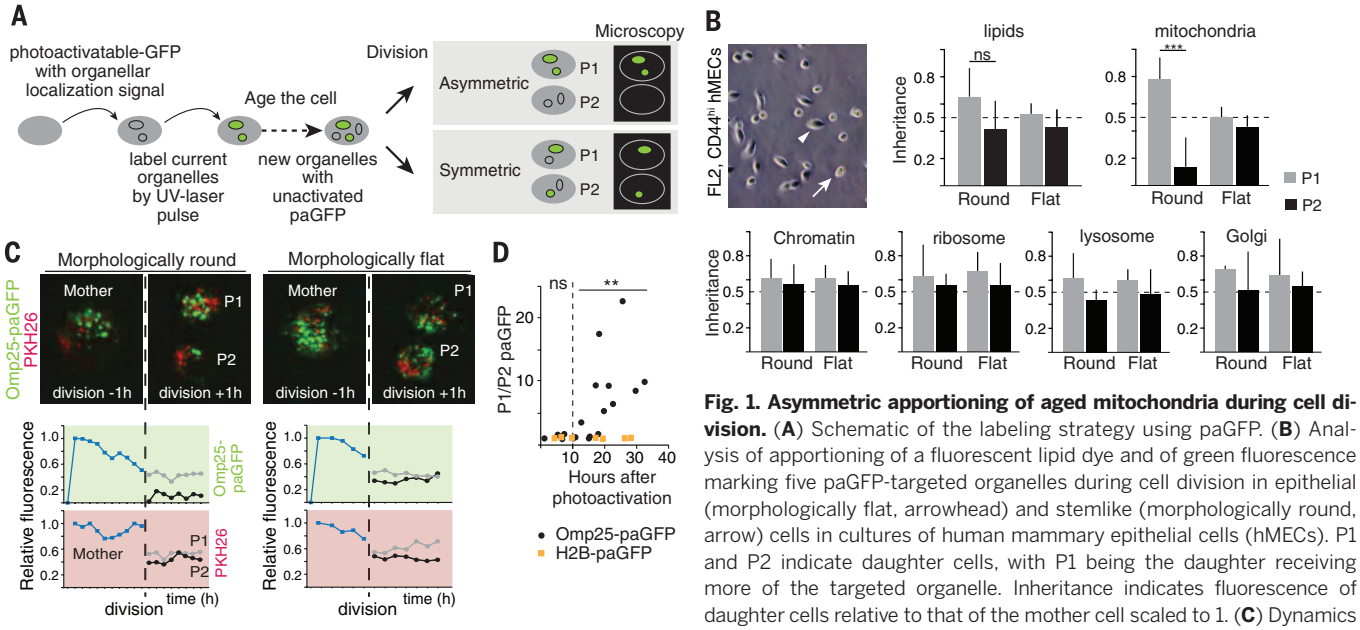

Fig. 1. Asymmetric apportioning of aged mitochondria during cell division. (**A**) Schematic of the labeling strategy using paGFP. (**B**) Analysis of apportioning of a fluorescent lipid dye and of green fluorescence marking five paGFP-targeted organelles during cell division in epithelial (morphologically flat, arrowhead) and stemlike (morphologically round, arrow) cells in cultures of human mammary epithelial cells (hMECs). P1 and P2 indicate daughter cells, with P1 being the daughter receiving more of the targeted organelle. Inheritance indicates fluorescence of daughter cells relative to that of the mother cell scaled to 1. (**C**) Dynamics of mitochondrial apportioning in round SLCs and flat epithelial cells. Representative divisions are shown with mitochondria in green (paGFP-Omp25) and the lipid dye (PKH26) in red. Images are frame captures from 1 hour before and after division, and fluorescence intensity per cell is plotted at 1-hour intervals. (**D**) Analysis of asymmetric apportioning as a function of label age. SLCs dividing more than 10 hours after label activation show increasing asymmetric apportioning of mitochondria (Omp25) but not of chromatin label (H2B). Each data point represents an individual cell division (**$P < 0.01$, ***$P < 0.001$, *t* test).

In this assay, the Pop2 of both Snap-Omp25– and COX8a-Snap–expressing cells formed three times as many mammospheres per 1000 cells as Pop1 (Fig. 3B). Hence, the cells that inherited fewer old mitochondria during an asymmetric division were, by the criterion of mammosphere-forming ability, more stemlike.

Mitochondria that have lower membrane potential (ΔΨm)—an index of mitochondrial function—localize perinuclearly (*18*), and high ΔΨm is linked to stemlike traits (*19*, *20*). Moreover, in *Saccharomyces cerevisiae*, the ΔΨm-driven selective inheritance of fit mitochondria is required for the daughter cell to maintain full replicative life span (*21*, *22*). We analyzed the ΔΨm of cells in the Pop1 and Pop2 populations to address whether their mitochondria differ functionally. Because the results with two different ΔΨm indicator dyes were not consistent (fig. S10), we analyzed the age-selective apportioning of mitochondria in the presence of a mitochondrial uncoupler, carbonyl cyanide *m*-chlorophenyl hydrazone. Alterations of the ΔΨm had no effect on the age-selective segregation of mitochondria in an SLC division (figs. S11 and S12). However, we did note a significant correlation between mammosphere-forming capacity and ΔΨm with both dyes (fig. S10). Thus, we conclude that although ΔΨm correlates with stemlike properties, it is not the signal that guides the age-selective asymmetric segregation of mitochondria during mammalian cell division.

Cells have mitochondrial quality-control mechanisms through which they specifically remove poorly functional parts of their mitochondrial network. After mitochondrial fission, which depends on the dynamin-related protein 1 (Drp1) (*23*), the kinase PINK1 will promote the recruitment of the Parkin E3 ubiquitin ligase to mitochondrial fragments with low ΔΨm and induce their selective autophagy (*24*). Another PINK1/Parkin-dependent (but ΔΨm- and Drp1-independent) mitochondrial quality-control mechanism is mediated by generation of mitochondrially derived vesicles that target oxidatively damaged mitochondrial components for lysosomal degradation (*25*).

SLCs and epithelial cells had comparable numbers of autophagosomes containing old mitochondrial label (fig. S13), indicating that degradation via the autophagosome-lysosome pathway is not directly responsible for the reduction in the numbers of old mitochondria in stemlike cells. However, SLCs had a higher mitophagy/autophagy ratio (fig. S13E), suggesting that high quality of mitochondria may be relevant for the SLC state and asymmetric apportioning during cell division. To investigate this, we transfected synchronized cells with small interfering RNAs (siRNAs) targeting Parkin or treated cells with the Drp1 inhibitor mDivi-1 (*26*) to inhibit mitochondrial fission. In both cases, we observed a significant and similar reduction in the number of cells inheriting mostly young mitochondria (Pop2) and a concomitant increase in cells inheriting a mixture of old and young mitochondria (Pop1) (Fig. 4A and fig. S14). Surprisingly, fragmentation of mitochondria by Drp1 expression resulted in comparable reduction in the Pop2 with mDivi-1 or siParkin (fig. S15). However, these effects are probably not caused by the changes of the mitochondrial network status, because round SLCs and differentiated cells have similar mitochondrial network connectivity (fig. S16 and movie S5). Taken together, these data suggest that any perturbation that challenges normal mitochondrial quality-control mechanisms will either serve as a signal for an SLC to stop asymmetric segregation of mitochondria or, alternatively, overload the capacity of the SLCs to effectively apportion old mitochondria asymmetrically.

To address whether the preferential acquisition of younger mitochondria contributed to maintenance of stem cell function, we analyzed the mammosphere-forming capacity of the cells remaining in Pop2 after a division in the presence of either siParkin or mDivi-1. Both treatments eliminated the increased stemness capacity of the remaining Pop2 cells so that they formed mammospheres with the lower efficiency characteristic of the Pop1 cells (Fig. 4B). However, the cells in Pop2 from mDivi-1–treated samples proliferated similarly to control-treated cells in 2D culture (fig. S14B). Moreover, because the analysis of mammosphere formation was conducted in the absence of mDivi-1, these data suggest that

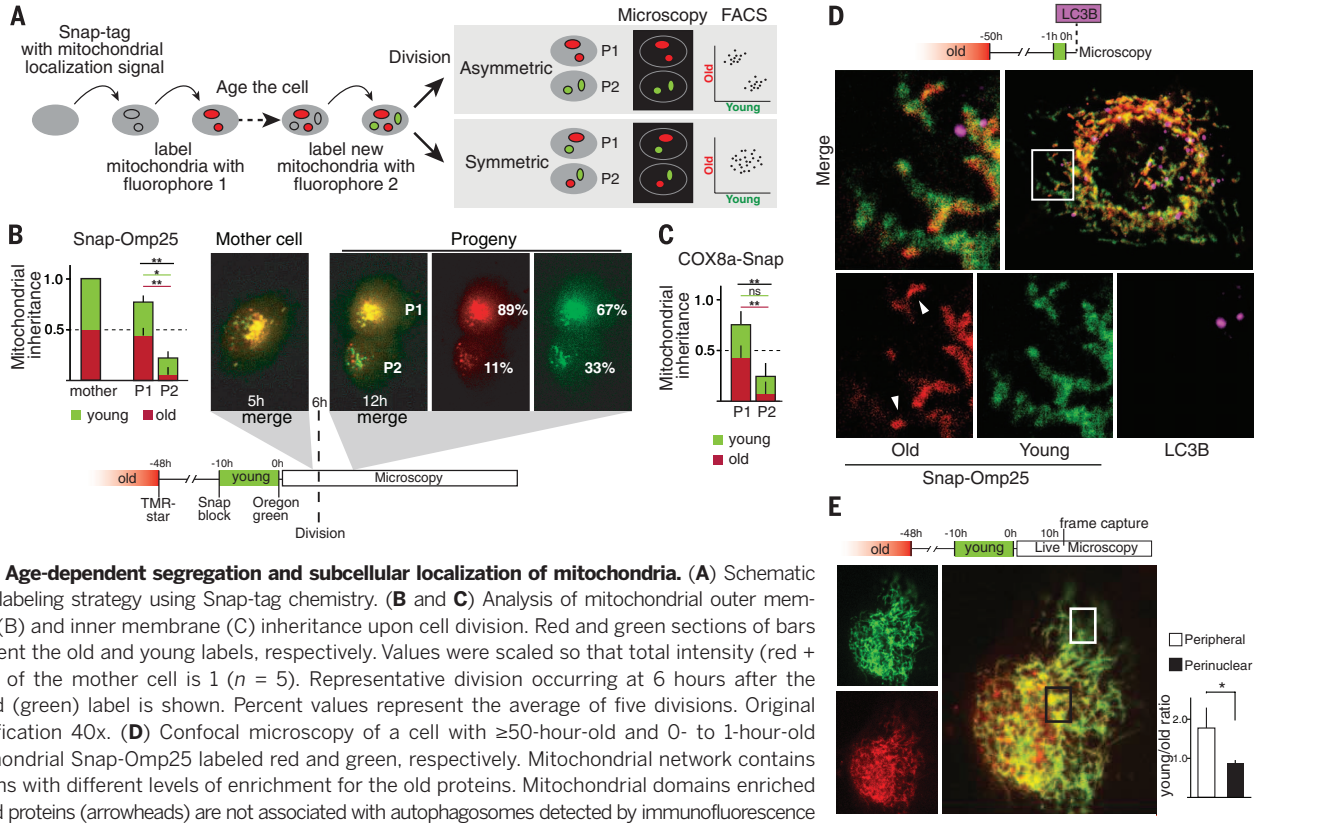

Fig. 2. Age-dependent segregation and subcellular localization of mitochondria. (**A**) Schematic of the labeling strategy using Snap-tag chemistry. (**B** and **C**) Analysis of mitochondrial outer membrane (B) and inner membrane (C) inheritance upon cell division. Red and green sections of bars represent the old and young labels, respectively. Values were scaled so that total intensity (red + green) of the mother cell is 1 (n = 5). Representative division occurring at 6 hours after the second (green) label is shown. Percent values represent the average of five divisions. Original magnification 40x. (**D**) Confocal microscopy of a cell with ≥50-hour-old and 0- to 1-hour-old mitochondrial Snap-Omp25 labeled red and green, respectively. Mitochondrial network contains domains with different levels of enrichment for the old proteins. Mitochondrial domains enriched with old proteins (arrowheads) are not associated with autophagosomes detected by immunofluorescence for LC3B (purple) (63x, 2 μm Z section). (**E**) Localization of old (red) and young (green) mitochondria (Snap-Omp25) 10 hours after labeling in an undivided cell. Squares mark regions used for measurements of the perinuclear and peripheral intensities in frames captured 10 hours after labeling for n = 3 (cells imaged from three separate labeling experiments) (*P < 0.05, **P < 0.01, t test).

the failure to asymmetrically apportion old mitochondria in a single division caused a persistent loss of stemness in SLCs.

To understand how alterations of mitochondrial dynamics and quality control might eliminate the age-selective apportioning, we administered mDivi-1 to cells 46 hours after labeling old mitochondria and followed the cells with live microscopy. The old mitochondrial label that had been confined to the perinuclear region spread throughout the mitochondrial network of the cell periphery after mDivi-1 administration (Fig. 4C, fig. S14C, and movie S4). Thus, stem cells normally confine mitochondria containing old proteins to distinct subcellular domains by a Drp1-dependent mechanism, and such age-dependent localization of old mitochondria may be required for their asymmetric apportioning.

Our approaches for studying age-selective asymmetry during cell division show that mammalian epithelial stemlike cells allocate their mitochondria age-dependently and asymmetrically between daughters upon cell division. The mechanisms involved require normal functioning of the mitochondrial quality-control machineries and mitochondrial fission that spatially restrict old mitochondrial matter to the perinuclear region of the mother cell. Because our work was conducted on mammary epithelial stemlike cells in vitro, future work addressing the extent of the phenomenon in other stem cell compartments and in vivo is needed. Interestingly, asymmetric cell division of mammalian embryonic stem cells depends on polarized paracrine signals (*27*) that could also further influence mitochondrial apportioning. Other recent evidence has implicated mitochondrial fitness in aging (*4*, *28*, *29*) and in tissue maintenance (*30*, *31*). It will be important to determine whether the age-dependent asymmetric apportioning of mitochondria described here has a role in such physiologic processes.

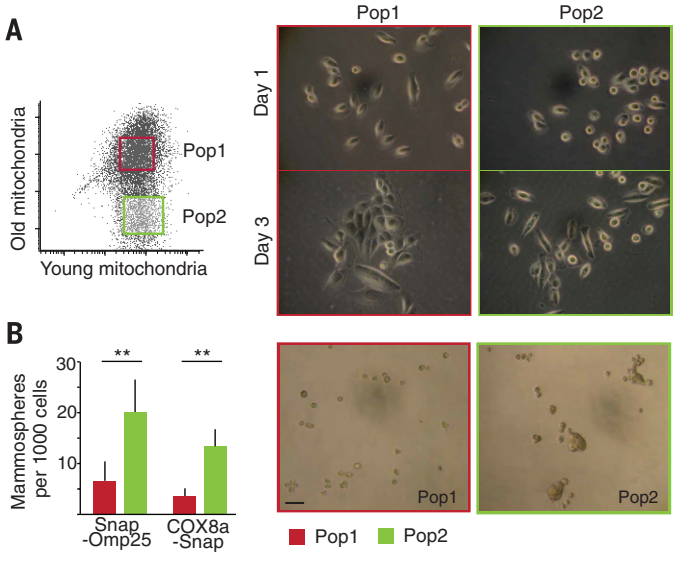

Fig. 3. Stemness properties of daughter cells receiving younger mitochondria. (**A**) FACS-mediated isolation of cell populations with high and low contents of old mitochondria (Pop1 and Pop2, respectively). Images show representative populations after 1 and 3 days in culture. (**B**) Mammosphere-forming capacity of Pop1 and Pop2 cells for $n = 5$ (scale bar, 50 μm; $^{**}P < 0.01$, t test).

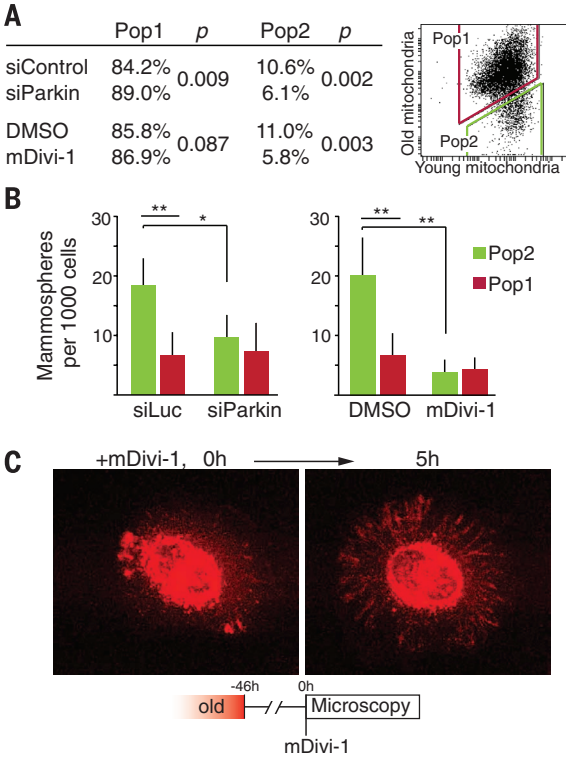

Fig. 4. Effects of mitochondrial quality control on asymmetric apportioning of old mitochondria during cell division. (**A**) FACS analyses of mitochondrial apportioning in cells with defective mitochondrial quality control induced by siRNA-mediated depletion of Parkin (siParkin) or pharmacological inhibition of mitochondrial fission (mDivi-1). Table presents the percentages of cells in the two populations for $n = 3$. (**B**) Mammosphere-forming capacity of cells in Pop1 and Pop2 are equal after siRNA Parkin and mDivi-1 ($n = 3$). (**C**) Localization of old mitochondria after treatment with mDivi-1. Images are frame captures at start (0 hours) and 5 hours after mDivi-1 administration. Original magnification 63x. ($^{*}P < 0.05$, $^{**}P < 0.01$, t test)

REFERENCES AND NOTES

1. D. J. Rossi *et al.*, *Nature* **447**, 725–729 (2007).
2. F. Coumailleau, M. Fürthauer, J. A. Knoblich, M. González-Gaitán, *Nature* **458**, 1051–1055 (2009).
3. P. Fichelson *et al.*, *Nat. Cell Biol.* **11**, 685–693 (2009).
4. J. R. McFaline-Figueroa *et al.*, *Aging Cell* **10**, 885–895 (2011).
5. H. Aguilaniu, L. Gustafsson, M. Rigoulet, T. Nyström, *Science* **299**, 1751–1753 (2003).
6. R. Spokoini *et al.*, *Cell Reports* **2**, 738–747 (2012).
7. M. A. Rujano *et al.*, *PLOS Biol.* **4**, e417 (2006).
8. M. Hernebring *et al.*, *Sci. Rep.* **3**, 1381 (2013).
9. D. Vilchez *et al.*, *Nature* **489**, 304–308 (2012).
10. C. L. Chaffer *et al.*, *Proc. Natl. Acad. Sci. U.S.A.* **108**, 7950–7955 (2011).
11. A. Raouf *et al.*, *Cell Stem Cell* **3**, 109–118 (2008).
12. G. H. Patterson, J. Lippincott-Schwartz, *Science* **297**, 1873–1877 (2002).
13. G. M. Lee, S. S. Fong, D. J. Oh, K. Francis, B. O. Palsson, *In Vitro Cell. Dev. Biol. Anim.* **38**, 90–96 (2002).
14. A. Keppler *et al.*, *Nat. Biotechnol.* **21**, 86–89 (2003).
15. G. Hernandez *et al.*, *Autophagy* **9**, 1852–1861 (2013).
16. K. A. Lukyanov, D. M. Chudakov, S. Lukyanov, V. V. Verkhusha, *Nat. Rev. Mol. Cell Biol.* **6**, 885–891 (2005).
17. G. Dontu *et al.*, *Genes Dev.* **17**, 1253–1270 (2003).
18. K. Okatsu *et al.*, *Genes Cells* **15**, 887–900 (2010).
19. C. Mantel, S. Messina-Graham, H. E. Broxmeyer, *Cell Cycle* **9**, 2008–2017 (2010).
20. A. Charruyer *et al.*, *J. Invest. Dermatol.* **132**, 2522–2533 (2012).
21. R. Higuchi *et al.*, *Curr. Biol.* **23**, 2417–2422 (2013).
22. C. Y. Lai, E. Jaruga, C. Borghouts, S. M. Jazwinski, *Genetics* **162**, 73–87 (2002).
23. E. Smirnova, L. Griparic, D. L. Shurland, A. M. van der Bliek, *Mol. Biol. Cell* **12**, 2245–2256 (2001).
24. C. Vives-Bauza *et al.*, *Proc. Natl. Acad. Sci. U.S.A.* **107**, 378–383 (2010).
25. G. L. McLelland, V. Soubannier, C. X. Chen, H. M. McBride, E. A. Fon, *EMBO J.* **33**, 282–295 (2014).
26. A. Cassidy-Stone *et al.*, *Dev. Cell* **14**, 193–204 (2008).
27. S. J. Habib *et al.*, *Science* **339**, 1445–1448 (2013).
28. A. L. Hughes, D. E. Gottschling, *Nature* **492**, 261–265 (2012).
29. S. M. Rafelski *et al.*, *Science* **338**, 822–824 (2012).
30. A. Vazquez-Martin *et al.*, *Aging* **4**, 393–401 (2012).
31. B. DuBoff, J. Götz, M. B. Feany, *Neuron* **75**, 618–632 (2012).

ACKNOWLEDGMENTS

We thank all members of the Sabatini and Katajisto laboratories—especially A. Efeyan, W. Comb, Y. Chudnovsky, and L. Schweitzer—for comments on this manuscript; K. Birsoy and E. Salminen for help and reagents; and K. Ottina for RNAi reagents. This work was supported by the U.S. National Institutes of Health (R01 CA103866, R01 CA129105, and R37 AI047389) (D.M.S.), Foundations' Post Doc Pool (P.K.), Academy of Finland (P.K.), Juselius Foundation (P.K.) and Marie Curie Actions (P.K.). D.M.S. is an Investigator of the Howard Hughes Medical Institute.

SUPPLEMENTARY MATERIALS

www.sciencemag.org/content/348/6232/340/suppl/DC1
Materials and Methods
Figs. S1 to S17
Table S1
Movies S1 to S5
References

25 August 2014; accepted 12 March 2015
Published online 2 April 2015;
10.1126/science.1260384

Science
AAAS

Asymmetric apportioning of aged mitochondria between daughter cells is required for stemness

Pekka Katajisto *et al.*

Science **348**, 340 (2015);
DOI: 10.1126/science.1260384

Science (print ISSN 0036-8075; online ISSN 1095-9203) is published weekly, except the last week in December, by the American Association for the Advancement of Science, 1200 New York Avenue NW, Washington, DC 20005.